Check for updates

Comparative investigation of the structural characteristics of tobacco stalk lignin during the DES and alkaline deconstruction toward sustainable materials

Na Wang[1], Bo Wang[1], Hui Si[1], Suxia Hu[1], Lin Chen[1], Yu Liao[1], Lei Wang[2]*, Yifan Zhang[2]* and Jungang Jiang[2]*

[1]China Tobacco Hubei Industrial Co., Ltd., Wuhan, China, [2]Hubei Provincial Key Laboratory of Green Materials for Light Industry, Hubei University of Technology, Wuhan, China

Lignin polymer as a natural aromatic macromolecule presents significant prospects in producing functional and sustainable materials, and achieving a comprehensive characterization will facilitate their target valorization. In the present study, deep eutectic solvent (DES) and alkaline delignification were adopted to deconstruct tobacco stalk before and after hydrothermal pretreatment, obtaining diverse lignin fractions with fascinating characteristics. DES lignin exhibited a higher yield and homogenous molecular structure than MWL. A severe cleavage of the inter-unit linkages in lignin was also observed. This result mostly originated from the efficient delignification of the DES deconstruction system adopted. Moreover, all the recovered lignin fractions exhibited good micro-nanoparticle size that can enhance the valorization of lignin in nanomaterial production, in which the hydrothermal-assisted DES deconstruction promoted the formation of the smaller lignin nanoparticle size. Next, all the recovered lignin presented an excellent UV absorption and structure-related absorption performance or thermal properties. Overall, this work provides an important foundation for further exploiting DES/alkaline delignification lignin that can be applied as an ideal feedstock for producing sustainable functional or micro/nanomaterials.

KEYWORDS

macromolecular structure, tobacco stalk, lignin, deep eutectic solvent, UV absorption

Introduction

Lignocelluloses, mainly consisting of cellulose, hemicelluloses, and lignin, are considered fantastic alternative feedstock for the replacement of petrochemical resources, owing to their abundance, eco-friendliness, and renewability, which can be converted into diverse fuels, materials, and fine chemicals (Zhang et al., 2017; Liu et al., 2019). Lignocellulosic biomass is also an excellent resource for the cooperative and sustainable development of the global green economy. Tobacco stalk is a kind of typical

waste biomass among various lignocellulosic feedstocks, which is generated from the agricultural industry (Wang et al., 2022). Tobacco stalk can be transformed into promising green energy and platform chemicals. However, this agricultural waste is always of low utilization, most of which is burned to generate heat, causing environmental pollution and wasting sustainable resources. Actually, lignin is an intricate heteropolymer that is cross-linked by various bonding motifs, for example, β-O-4, β-β, β-5, and β-1 (Ralph et al., 2004; Wang et al., 2017), and is a valuable resource that can be tailored into sustainable, functional materials (Laurichesse and Averous, 2014; Wang et al., 2020). However, the high recalcitrant and complex structures of tobacco stalk impede the utilization of components and conversion (Zhao et al., 2012). Thus, achieving effective deconstruction of lignocellulose is the principal step for lignin valorization.

According to the twelve principles of green chemistry, a biorefinery strategy should realize the high value-added utilization of biomass resources and adhere to the waste-free standpoint (Clarke et al., 2018). In recent years, some pretreatment methods such as physical, chemical, and biological pretreatment have been adopted to deconstruct different lignocellulosic materials (Clarke et al., 2018; Wang B. et al., 2018). Deep eutectic solvents (DESs) have attracted more and more attention as the potential green solvents for biorefinery with advantages such as easy synthesis, low cost, biodegradability, and low toxicity (Bjeli´c et al., 2020). DESs are generally prepared by hydrogen bond donors (HBDs) and hydrogen bond acceptors (HBAs), forming a stable and homogeneous solvent with desirable low cost and recyclability (Bjeli´c et al., 2020). At present, DES has been widely applied in the deconstruction of biomass, which can enhance the enzymatic hydrolysis rate of cellulose for sugar conversion and lignin dissociation (Hladnik et al., 2021; Wang et al., 2022). Among them, acidic and basic DESs exert efficient delignification toward various lignocelluloses, meanwhile neutral DES also showed great potential in lignin fractionation owing to its eco-friendliness and easy availability (Ma et al., 2021a; Wang et al., 2022). Alkaline DESs showed better structural retention for lignin macromolecules (Xu et al., 2021; Wang et al., 2022). However, the combination of glycerol (Gly) and choline chloride (ChCl) has an inferior ability to dissolve lignin (Alvarez-Vasco et al., 2016), whereas the addition of Lewis acids in the glycerol and choline chloride system could contribute to the satisfactory delignification of lignocellulose. This mainly originated from the proton-catalyzed linkage cleavage between lignin and matrix (Chen et al., 2020; Ma et al., 2021b). Actually, DES pretreatments can be adapted to isolate various lignin fractions that are promising materials for functional materials. Importantly, lignin extracted by the DES system can be utilized to fabricate different lignin-based materials, such as UV-blocking composite film, antioxidant polyethersulfone membranes, and lithium-ion batteries (Esmaeili et al., 2018; Guo et al., 2020; Vin-Nnajiofor. et al., 2022).

Recently, some studies have proved that polyalcohol-based DES systems, such as glycerol, ethylene glycol, and butanediol, exhibited ideal delignification efficiency for lignocellulose deconstruction (Chen et al., 2020; Cheng et al., 2022; Ma et al., 2022). It was reported that the isolation of lignin and the enhancement of enzymatic hydrolysis by various polyalcohol-based DES pretreatments were efficient by comprehensive investigation (Chen et al., 2018). These DESs can be used to enhance the production of high-yield fermentable sugars and tailored lignin nanoparticles and sustainably explore the strategy for the conversion of diverse biomass (Hladnik et al., 2021; Ma et al., 2022). Hydrothermal pretreatment (HTP), as an eco-friendly and economical technology, can not only improve hemicelluloses and obtain xylooligosaccharides (XOS) from biomass but also promote the deconstruction of lignocellulose (Wang et al., 2019a). The combination of HTP and DES is an excellent and green strategy for the valorization of lignocellulose, in which the structural characteristics of lignin during the deconstruction process are important for their value-added conversion into sustainable materials. Therefore, comprehensively investigating lignin structures is a precondition for lignin valorization. Alkaline delignification is a typical approach for deconstructing lignocellulose, and most of the industrial lignin that originate from this process is an ideal precursor for producing functional materials. Presently, no study has been performed to investigate the structural differences of lignin between DES pretreatment and alkaline delignification. Knowing their structural characteristics will guide the fabrication of lignin-based materials.

In the present study, DES deconstruction (ChCl–ethylene glycol–$AlCl_3 \cdot 6H_2O$/ChCl–glycerol–$AlCl_3 \cdot 6H_2O$) and alkaline delignification were applied to dissociate raw and hydrothermal tobacco stalk, acquiring different lignin fractions that were used to comparatively explore their structural features, such as lignin yield and lignin structures. Moreover, the structural changes of lignin during the DES pretreatment were comparatively elucidated by 2D-HSQC NMR and FTIR techniques compared to MWL from raw tobacco stalk. In addition, the micro-nano morphology and ultraviolet-visible light adsorption, as well as thermostability, were investigated. It is believed that the comprehensive characterization of lignin from DES deconstruction and alkaline delignification will boost the lignin valorization and further facilitate the exploitation of bio-based materials.

Materials and methods

Materials

Tobacco stalks were kindly provided by the Institute of Tobacco Science and Technology (Zhengzhou, China). Topically, tobacco stalks were cut into 3–5 cm length, then

FIGURE 1
Scheme of tobacco stalk dissociation and lignin isolation.
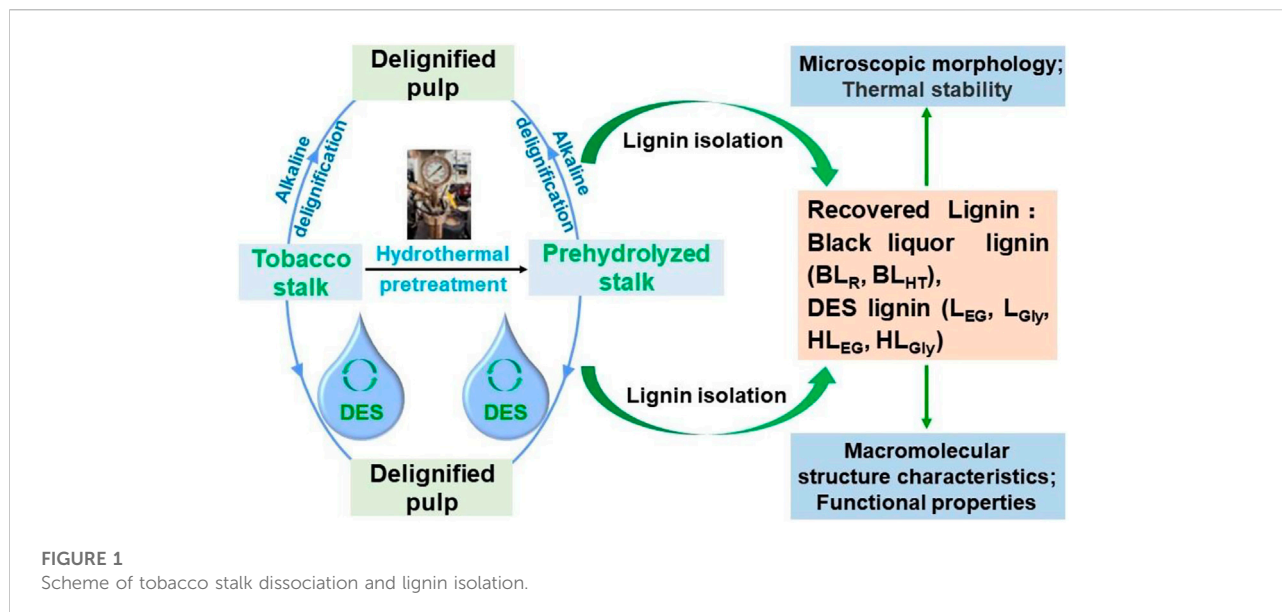
milled into 40–60 mesh powder, and oven-dried at 60°C for 48 h. Chemical compositions of the stalk are cellulose (40.5 wt%), hemicelluloses (21.5 wt%), lignin (22.3 wt%), and others (15.7 wt%), which are determined according to the National Renewable Energy Laboratory (NREL) method (Sluiter et al., 2008). Hydrothermal pretreatment (HTP) of tobacco stalk was performed in a stainless-steel reactor (Parr, United States) with a solid-to-liquid ratio of 1:8 (g/ml) at 170°C for 1 h (Wang et al., 2019b). Afterward, the treated tobacco stalks were separated by nylon gauze and oven-dried (60°C) to obtain HTP tobacco stalk. Choline chloride (ChCl), ethylene glycol (EG) or glycerol (Gly), aluminum chloride hexahydrate (AlCl$_3$·6H$_2$O), acetone (analytical grade), and sodium hydroxide (NaOH) were purchased from Sigma Chemical Co., Ltd.

Preparation of DES

Two DESs were synthesized by mixing the pre-dried choline chloride (ChCl), ethylene glycol (EG) or glycerol (Gly), and aluminum chloride hexahydrate (AlCl$_3$·6H$_2$O) at a molar ratio of 1:2:0.1 under constant stirring at 80°C for 1 h (Ma et al., 2021a). The prepared transparent DES solvents were stored in a desiccator prior to use.

DES pretreatment and alkaline delignification

The general scheme of deconstruction of tobacco stalk through DES pretreatment and alkaline delignification is depicted in Figure 1. In detail, the DES pretreatments of

tobacco stalk were performed using a mixing ratio of 1:10 (w/w, tobacco stalk powder:DES) in a 50 mL round-bottom flask, which was heated in an oil bath raised (with a heating rate of 10°C/min) from room temperature to 120°C and held for 4 h. For HTP tobacco stalk, all the conditions were similarly adopted as mentioned earlier, except for the held time (2 h). All the conditions adopted in this work were based on previous studies (Ma et al., 2021b; Wang et al., 2022). After the DES pretreatment, acetone/water (50 ml, 1:1 v/v) solvent was poured into the resultant dark-brown liquid with stirring for 10 min to terminate the reaction. The mixture was vacuum-filtered and washed with the same acetone/water solvent three times to remove the residual DES. Then, all the filtrates were mixed and heated in a rotary evaporator at 50°C to remove acetone, and the recovered solids were centrifuged to obtain DES lignins, which were named L$_{EG}$, L$_{Gly}$, HL$_{EG}$, and HL$_{Gly}$, respectively.

Meanwhile, raw and HTP tobacco stalks were also subjected to alkaline delignification to obtain black liquor lignin (BL), aiming to comparatively investigate the structural characteristics between DES lignin and BL. Alkaline delignification of tobacco stalks was carried out under the following conditions: 20 wt% alkali charge (16 wt% for HTP tobacco stalks), 0.5 wt% anthraquinone (AQ) charge, solid-to-liquid ratio 1:5 (g/ml), and 140°C for 1 h (21). After cooking, black liquor and solid residue were separated by filtrating with a nylon bag, and the black liquor was collected to isolate lignin samples. For example, black liquor from raw and HTP tobacco stalks was dropped into the acidic water (pH 2) under continuous magnetic stirring to precipitate BLs, which were labeled as BL$_R$ and BL$_{HT}$, respectively. Parallelly, the native lignin milled wood lignin (MWL) from raw tobacco stalk was also isolated to investigate

TABLE 1 Yields and weight-average (Mw), number-average (Mn) molecular weights, and polydispersity index (PDI, Mw/Mn) of lignin samples (g/mol).

Sample	Yield (%)	Sugar content (%)	Mw	Mn	PDI
MWL	35.6 ± 1.1	3.4	2,580	2,010	1.3
L_{EG}	56.5 ± 0.8	1.5	3,050	3,000	1.0
L_{Gly}	50.3 ± 1.2	3.1	2,410	2,350	1.0
HL_{EG}	65.1 ± 0.9	0.8	2,130	1,710	1.2
HL_{Gly}	53.4 ± 1.5	2.8	1,880	1,860	1.0
BL_R	74.6 ± 1.5	3.5	2,470	2,370	1.1
BL_{HT}	80.3 ± 1.8	2.0	2,790	2,800	1.0

the structural changes of lignin during DES deconstruction and alkaline delignification (Björkman, 1954).

Analysis methods of the lignin samples

In order to comprehensively compare the macromolecular structural characteristics of lignins, different characterization techniques were applied. Gel permeation chromatography (GPC, Agilent 1200, United States) equipped with a refractive index detector was used to detect the number-average (Mn) and weight-average (Mw) molecular weights of the lignin fractions (Wang et al., 2017). The Bruker AVIII 400 MHz spectrometer (Bruker, Germany) was adopted to collect the quantitative 2D-HSQC spectra of the lignin dissolved in DMSO-d_6 (Rencoret et al., 2008; Wen et al., 2013a; Wang et al., 2017). Thermal stability and functional characteristics (i.e., UV-vis absorption) of these lignin samples were also assessed with a DTG analyzer (DTG-60, Shimadzu, Japan) and UV spectroscopy (UV-2550, Shimadzu, Japan) as previously (Wang et al., 2022). In addition, a scanning electron microscope (SEM, SU8010) was selected to observe the microscopic morphology of the recovered lignin fractions to guide their further application.

Results and discussion

Yields and molecular weight distributions of lignin

Lignin yield (based on Klason lignin) is an important criterion for assessing the effectiveness of the lignocellulose deconstruction, which is also crucial for the structural characterization of lignin. MWL is the typical native lignin that can reveal the representative structures of raw lignin samples from lignocellulose. In this study, all the yields of the lignin samples are listed in Table 1. MWL presented the lowest yield of 35.6%, which prominently originated from the high

recalcitrance of raw tobacco stalk (Pu et al., 2013). In contrast, lignin samples from DES deconstruction and alkaline delignification showed a significant enhancement (ranging 50.4%–80.3%) compared to that of MWL, indicating that these deconstruction processes were efficient for tobacco stalk, and the biomass recalcitrance was effectively disrupted. Among them, alkaline delignification processes dissociate the higher amount of lignin, suggesting that traditional alkaline pulping is an efficient pathway for lignocellulose delignification. BL_{HT} showed a higher yield than BL_R due to the pre-subjected HTP process that can partially dissociate the rigid matrix of biomass (Li et al., 2018). Similarly, an identical phenomenon was also observed in DES lignins (Table 1). Furthermore, the recovered yield of lignin from the ChCl/EG system was slightly higher than that of the ChCl/Gly system, indicating that ChCl/EG exhibited more obvious delignification efficacy for this tobacco stalk. In addition, the sugar contents in the lignin fractions showed that BLs had more carbohydrates than those of DES lignins, which also can be verified by the following 2D HSQC spectra.

Molecular weights of different lignin samples have also been recorded by the GPC technique, and the relative results are listed in Table 1, in which L_{EG} and L_{Gly} showed larger molecular weights (3,050 and 2,410 g/mol, respectively) than HL_{EG} and HL_{Gly} (2,130 and 1,880 g/mol, respectively). In fact, the HTP process plays a vital role in depolymerizing lignin polymer that partially reduces the molecular weights of HL_{EG} and HL_{Gly} (Li et al., 2018; Wang et al., 2019a). Moreover, BLs showed relatively minor molecular weights suggesting that lignin macromolecule was also greatly depolymerized during the alkaline cooking procedure. Notably, the PDI of all the recovered lignin samples narrowly ranged 1.2–1.0. This implied that these lignin fractions were extremely homogenous polymers that can be targeted into various lignin-based products, such as lignin-derived functional or nanomaterials (Sajjadi et al., 2021; Wang et al., 2021). It was reported that the lignin with lower molecular weights normally contained significant amounts of functional groups, such as hydroxyl and carboxyl groups (Laurichesse and Averous, 2014), and these characteristics will encourage the upgrading of the lignin polymers.

2D-HSQC NMR spectra of lignin

The advanced 2D-HSQC NMR technique was applied to characterize lignin (Rencoret et al., 2008; Wen et al., 2013b). The obtained 2D-HSQC spectra of these lignin samples from tobacco stalk are presented in Figure 2, and the quantitative results of linkages are also listed in Table 2.

The side-chain region of 2D-HSQC spectra from these lignin samples showed the diverse linkages present in the lignin macromolecules (Figure 2). For the MWL from tobacco stalk, a typical 2D-HSQC spectrum of native lignin was observed that the main linkages, such as β-O-4 linkages (A), β-β linkages (B),
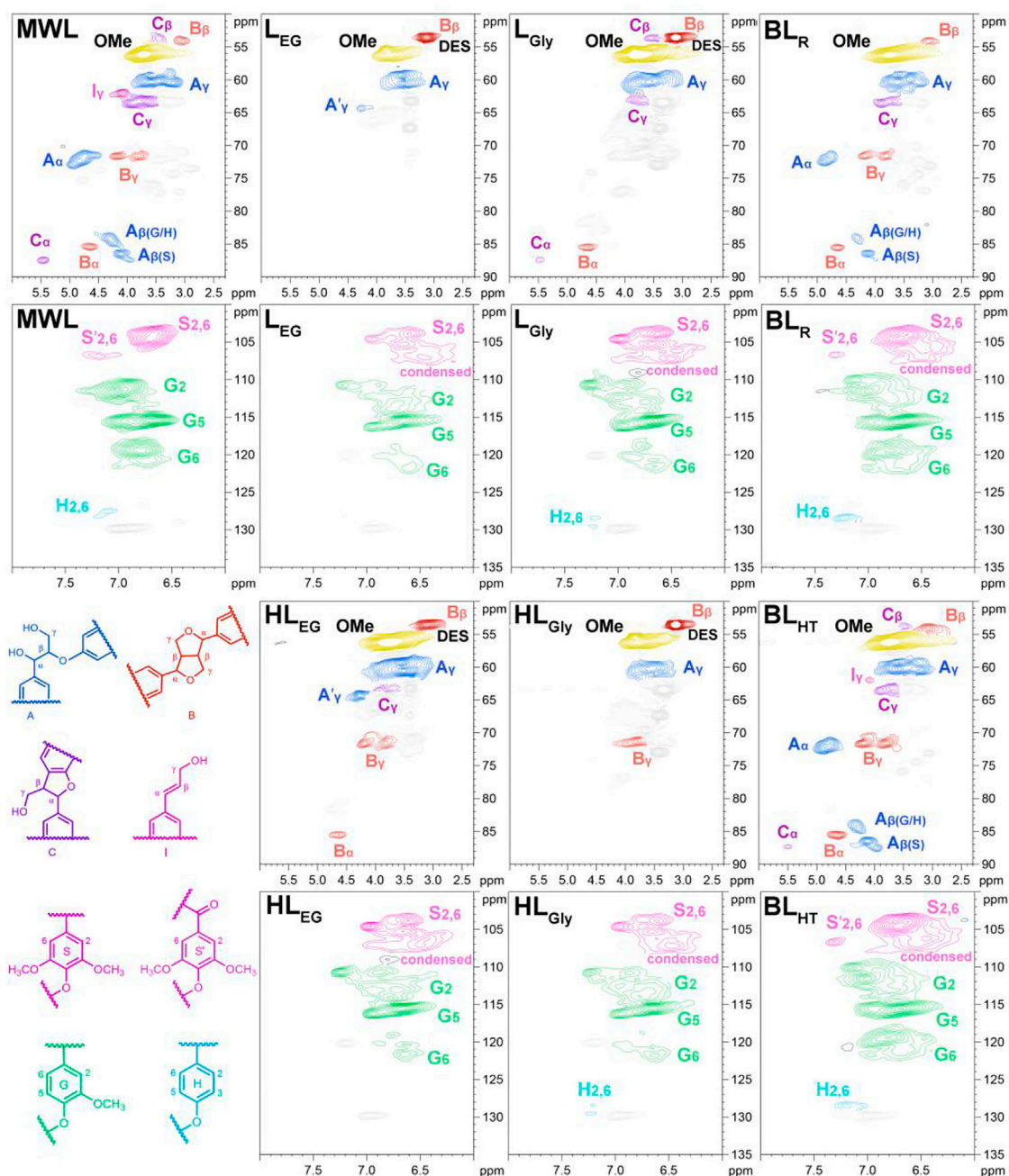
FIGURE 2
2D-HSQC spectra of different lignin samples and the identified linkages.

and β-5 linkages (C), with three obvious chemical shifts (α, β, and γ positions), can be clearly assigned based on previous literature (Wen et al., 2013a; Wang et al., 2017; Wang et al., 2022). Then, *p*-hydroxycinnamyl alcohol end groups (I) also can be identified with strong signal intensity. However, the lignin fractions from DES pretreatment and alkaline cooking showed severely destroyed structures, in which most of the linkages were

disrupted and disappeared in the spectra (especially for DES lignins), which definitely resulted from the crushing conditions during these delignification processes (Ma et al., 2022). It was also noted that BLs showed a relatively integrated structure compared to other DES lignins. This phenomenon can be attributed to the fact that aqueous alkaline solvent has an excellent swelling effect on lignocellulose and has little effect on the lignin structures

**TABLE 2** Quantification of lignin samples by the quantitative 2D HSQC method.

| Sample	β-O-4	β-β	β-5	S/G
MWL	49.5	8.0	5.2	0.5
L_{EG}	ND	ND	ND	0.5
L_{Gly}	ND	3.3	1.0	0.6
HL_{EG}	ND	ND	ND	0.6
HL_{Gly}	ND	ND	ND	0.5
BL_R	13.4	4.2	0.4	0.6
BL_{HT}	17.5	5.1	0.7	0.9

(typical substructures), leading to more lignin fractions efficiently dissolved and presenting high structural intensity (Wen et al., 2015; Sun et al., 2019). Furthermore, the γ-acetylated β-O-4 linkages (A′) occurred in the 2D-HSQC spectra of L_{EG} and HL_{EG}, owing to the acylation reaction that occurred in the lignin side chain under the given conditions.

In the aromatic region of 2D-HSQC spectra (Figure 2), signals from the syringyl (S), guaiacyl (G), and p-hydroxyphenyl (H) units were clearly distinguished in MWL (Rencoret et al., 2008). After the delignification process, the recovered lignin showed a relatively lower signal intensity and obvious condensed signals in S units (such as L_{EG} and HL_{EG}). It was found that H units disappeared in L_{EG} and HL_{EG}, and different reductions of signal intensities were also observed in other lignin samples. As mentioned earlier, BL_R and BL_{HT} also presented the relative integrity signals that the main S, G, and H units still contained, except for the occurrence of condensed signals at S units. In fact, condensation reaction also occurred in G units, as proved in the 2D-HSQC spectra (Figure 2). It has been

reported that condensation reactions occur not only at the 2, 5, and 6 positions of G units but also happen at the 5-position of other aromatic rings and Cα of lignin side-chains (Torr et al., 2012; Shen et al., 2019). In this study, the chemical shifts of G units (especially G2 and G6) were changed during DES pretreatment, which resulted from the formation of intricate C-C linkages during acid-catalyzed condensation (Torr et al., 2012). Additionally, it was noted that these lignin samples isolated from tobacco stalk showed no p-hydroxycinnamate (PCA and FA) structures, which is similar to hardwood lignin (SGH-type lignin) (Rencoret et al., 2008; Sun et al., 2019).

The quantitation of these 2D-HSQC spectra was acquired and presented in Table 2. As expected, the content of β-O-4 linkage in MWL was abundant compared to the other recovered lignin, which was 49.5/100 Ar. Also, BL_R and BL_{HT} exhibited minor amounts of β-O-4 linkages (13.4 and 17.5/100 Ar) that confirmed their structural integrity, as reflected in Figure 2. Lignin macromolecule with more β-O-4 linkage usually has a larger molecular weight and relatively intact structure. In the present study, MWL exhibited ideal structural integrity, and the molecular weight was similar to BL_R (2,580 vs. 2,470 g/mol), while BL_{HT} exhibited a higher molecular weight (2,800 g/mol) that mostly was attributed to the severe condensation reaction of lignin during the HTP process. For the DES lignin fractions, no visible linkages can be detected and only trace amounts of C-C linkages (e.g., β-β and β-5) were found in L_{Gly} (Table 2). In this study, MWL and DES lignin samples exhibited similar S/G ratio values even if the treated lignins had no raw linkages, and this result was caused by the obvious condensation that the units were linked by C-C linkages during the harsh condition. However, the higher S/G ratio values of BLs could be explained by demethoxylation during the alkali delignification (Wang et al., 2019b). Scheme 1 lists

SCHEME 1
Potential pathway for the lignin structural transformation during the delignification.
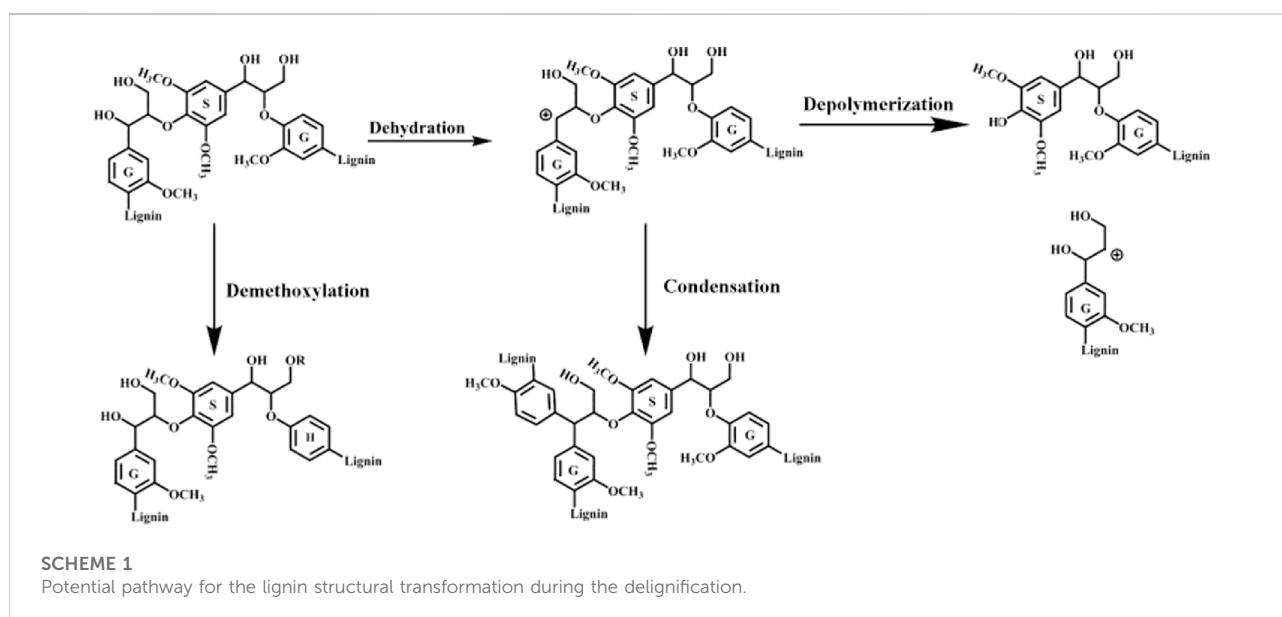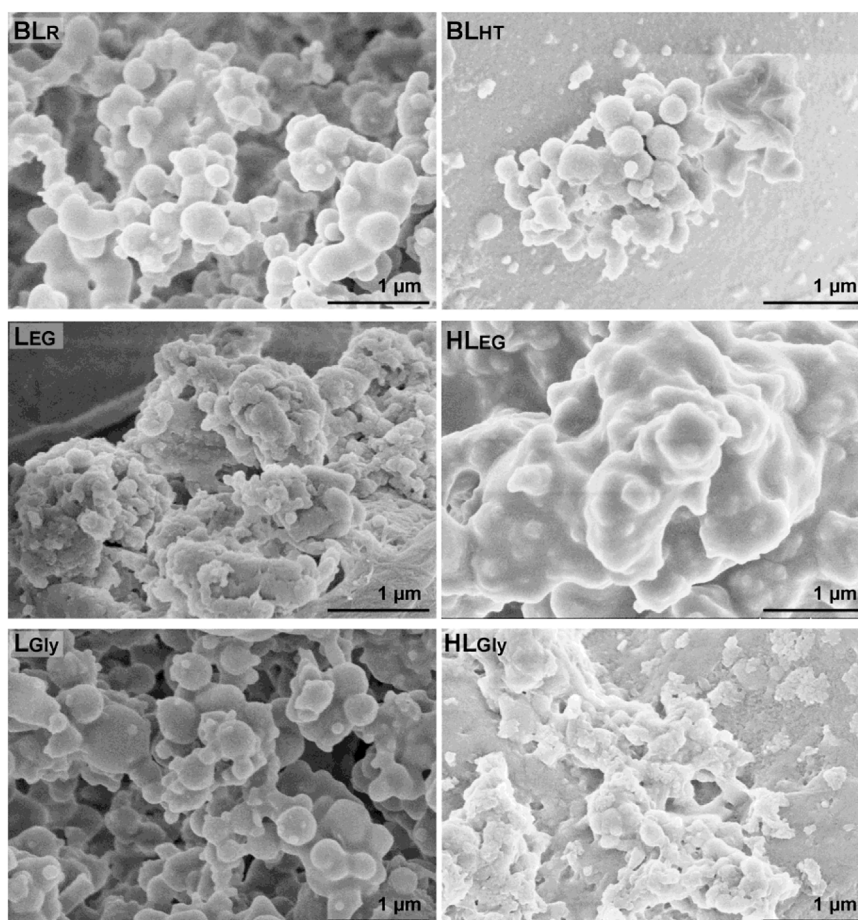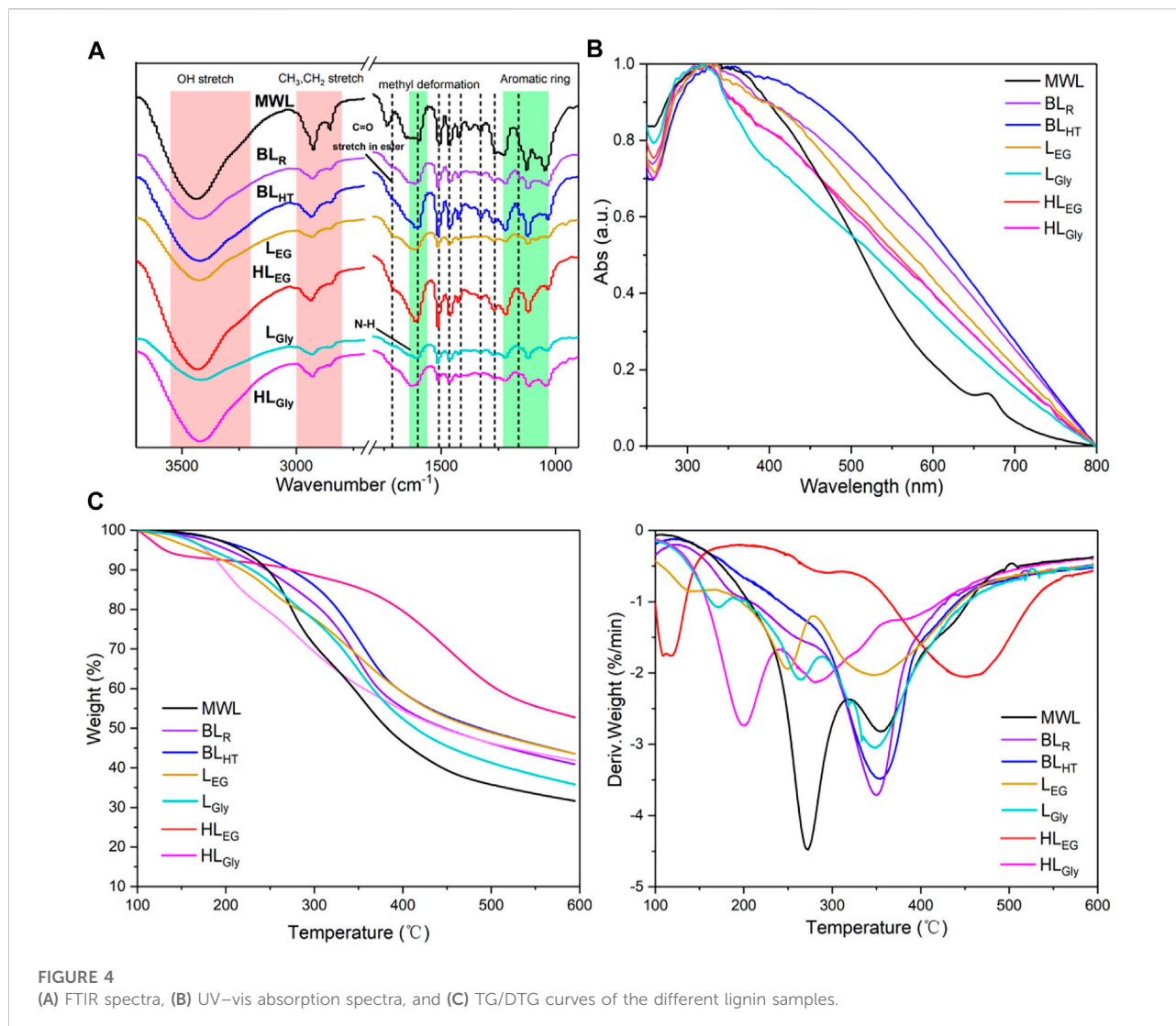
FIGURE 3
SEM images of sub-micron spheres from recovered lignin fractions.

the potential pathway for the lignin structural transformation during this delignification (Shen et al., 2019; Wang et. al., 2019a).

Micromorphology of the lignin

Recently, lignin nanoparticles or colloidal lignin particles have attracted increased attention, and some reports envision that lignin nanoparticles will have an important influence on promoting lignin valorization, such as the development of synthetic nanoparticles in the polymer industry (Zhao et al., 2016). Indeed, lignin micro-nanoparticles also possess outstanding antioxidant, UV-absorbing, and antimicrobial properties, which can be converted into sustainable biomedical materials, nanocomposites, and functional materials (Wang H et al., 2018; Monika et al., 2020; Siavash and Rajender, 2020). In this study, the micromorphology of the lignin fractions was investigated by scanning electron microscope (SEM), and the SEM images of sub-micron lignin spheres are

presented in Figure 3. It can be observed that BLs presented some regular micro-nanoparticles with different sizes, suggesting that lignin was well self-assembled during the recovery process from black liquor (Xu et al., 2022). Then, the recovered DES lignin also exhibited a micro-nanoparticle shape, in which the L_{EG} and L_{Gly} showed a relatively regular and large micro-nanoparticle shape. However, the HL_{EG} and HL_{Gly} presented the remarkable agglomeration of lignin. The severe agglomeration phenomenon of HL_{EG} and HL_{Gly} is probably owing to the HTP process that resulted in the condensed reaction of lignin (especially for HL_{EG}). Furthermore, HL_{Gly} also showed the smaller size of nanoparticles, which was in line with its lower molecular weight, as stated in Table 1. All the aforementioned results confirmed that the inherent structures of lignin would play a crucial role in the formation of lignin microtopography during the recovery procedure. Therefore, these DES lignins and BLs are exactly promising in fabricating lignin nanoparticles and lignin-based materials, which will deeply promote lignin conversion in the current green and sustainable biorefinery.

FIGURE 4
(A) FTIR spectra, **(B)** UV−vis absorption spectra, and **(C)** TG/DTG curves of the different lignin samples.

FTIR analysis of lignin

Figure 4A illustrates the FTIR spectra of all the lignin samples, which were assigned based on the previous literature (Dong et al., 2019). It could be observed that the peaks ranging 1,350–1,050 cm^{-1} of the FTIR spectra were attributed to the signals' vibration of the aromatic ring in lignin. The absorption peak located at 1,162 cm^{-1} is responsible for the esterified lignin (Christopher et al., 2019; Zhong et al., 2021), and MWL showed a strong absorption peak here, suggesting that more esterified linkages exist in MWL; that is, MWL had a high structural intensity. Next, the absorption peaks at 1,603, 1,510, 1,465, and 1,415 cm^{-1} were also attributed to the aromatic ring vibration and methyl deformation of lignin. Among them, the spectra of MWL exhibit a strong absorption peak around 1,750 cm^{-1} that originated from the C=O stretch ester of native lignin.

Obviously, the abundant peaks at 2,800–3,000 cm^{-1} for methyl and methylene groups of the MWL skeleton could be easily identified as compared with the other lignins, and this result indicated that the lignin polymer was significantly depolymerized during these DES pretreatment and alkaline delignification processes (Wang et al., 2022). In this study, lignin was extracted from tobacco stalk by the effective cleavage of lignin–carbohydrate linkages (LCC) and then dissolved in DESs and alkaline solvents (Wang et al., 2019b; Shen et al., 2019). In practice, some chemical reactions (e.g., depolymerization and condensation) occurred in lignin macromolecule and resulted in the more complex structures under given conditions (Zhong et al., 2021), which will restrict their utilization and targeted conversion. Therefore, exploring the applicable properties of the lignin is of significance for its value-added valorization, such as abundant functional groups, UV absorption, and high thermostability (Wang et al., 2022).

Ultraviolet light absorption and thermal stability of lignin

The existence of functional groups in lignin, such as phenolic hydroxyl groups and aromatic rings or conjugated double bonds, fatefully endows lignin with brilliant UV light absorption that could largely enhance the scope of practical application. Naturally, the UV absorption features of the lignin are also related to its macromolecular structure (Wang et al., 2022). In this study, the UV–vis absorption spectra of all the lignin samples were acquired, as shown in Figure 4B; it can be observed that all the lignin samples showed prominent absorption capacity toward UV light, suggesting that these have ideal UV absorption property. MWL showed the weaker absorption property was mostly related to its less functional groups (e.g., hydroxyl groups) in lignin polymer than that of other lignin fractions. Interestingly, BL_R and BL_{HT} exhibited the analogical spectra toward light absorption, and a similar phenomenon was also noticed for HL_{EG} and HL_{Gly}. The aforementioned results subtly indicated that lignin possessed identical structures that would show similar UV–vis absorption (Wang et al., 2022), whereas L_{EG} and L_{Gly} had different spectra mostly owing to their structural differences in the abundances of linkages and units, as shown in Figure 2. The promising UV absorption features of these lignin polymers revealed significant prospects in producing lignin-based UV-shielding materials (Monika et al., 2020; Wang et al., 2020), which could boost the upgrading feasibility of lignin in a sustainable pathway.

It has been reported that lignin structural characteristics play an important role in subsequent conversion and material properties of products, such as functional or carbon materials (Zhang et al., 2019; Xi et al., 2020b; Wang et al., 2021). Hence, investigating the thermal stability of lignin is vital for its subsequent conversion into value-added carbon materials and thermoplastic materials (Sanghamitra et al., 2015). The present study analyzed all the lignin samples by thermogravimetric analysis (TGA) to reveal the correlation between structural characteristics and thermal stability. Figure 4C shows that TG/DTG curves of the lignins are presented. Notably, the thermal degradation behavior of different lignin samples was diversiform, which was influenced by their inherent structures, that is, the chemical linkages, the abundance of functional groups, and the degree of condensation (Liu et al., 2021; Wang et al., 2022). It has been reported that the thermal decomposition behavior of lignin polymer was correlated to its molecular weight, whereas an inconspicuous tendency was found in this study, and this could be explained by their little differences in molecular weights (Table 1). Detailedly, MWL had the lowest content of residual char compared to the other treated lignin fractions, as shown in TGA (Figure 4C, left), which can be attributed to its abundant ether bonds and minor condensed linkages. It was observed that a slight reduction of weight before 200°C occurred in these lignin samples owing to the dehydration of the lignin macromolecule and weak or labile linkages disrupted. Then, the mass loss of lignins was drastic with the temperature increased up to 350°C. This change may be attributed to the side chain oxidation of lignin under high temperatures. As the temperature further enhanced, the rates of mass loss of lignin samples were visibly weak compared to the front period, in which C–C bonds and aromatic ring collapsed and sedimented into residual char. Finally, it was noticeable that almost lignin fractions showed a relatively high content of residual char (exceeding 40%), implying that these lignin polymers are excellent feedstock for the fabrication of carbon materials.

Conclusion

The present study adopted DES and alkaline delignification to deconstruct tobacco stalk before and after hydrothermal pretreatment, achieving different lignin fractions with various structural characteristics. Two kinds of DES isolated lignin polymer with higher yields and homogenous molecular structure compared to MWL. DES deconstruction of tobacco stalks resulted in the obvious disruption of linkages in lignin compared to those of black liquor lignins (BLs), mostly owing to the efficient delignification of DES and ideal dissolution of lignin in the alkaline solvent. Moreover, the recovered lignin fractions exhibited good micro-nanoparticle size that will significantly enhance the valorization of lignin in fabricating nanomaterials, in which the lignins from hydrothermal-assisted DES deconstruction presented the smaller nanoparticle size that mostly originated from their reduced molecular weights. Furthermore, all the recovered lignin showed excellent UV absorption and had a structure-induced absorption performance or carbon content. All these features promote these lignin fractions serving as great feedstock for producing sustainable functional or carbonaceous materials.

Data availability statement

The original contributions presented in the study are included in the article/supplementary material. Further inquiries can be directed to the corresponding authors.

Author contributions

NW: conceptualization, methodology, investigation, validation, and writing-original draft. BW: software, visualization, and validation. HS: software and visualization. SH: formal analysis and data curation. LC: formal analysis and data curation. YL: resources and formal analysis. LW: conceptualization, methodology, writing—review and editing,

and funding acquisition. YZ: resources, visualization, writing—review and editing, and project administration. JJ: conceptualization, methodology, writing—review and editing, and supervision.

Conflict of interest

NW, BW, HS, SH, LC, and YL were employed by China Tobacco Hubei Industrial Co., Ltd.

The remaining authors declare that the research was conducted in the absence of any commercial or financial

relationships that could be construed as a potential conflict of interest.

Publisher's note

All claims expressed in this article are solely those of the authors and do not necessarily represent those of their affiliated organizations or those of the publisher, the editors, and the reviewers. Any product that may be evaluated in this article, or claim that may be made by its manufacturer, is not guaranteed or endorsed by the publisher.

References

Alvarez-Vasco, C., Ma, R., Quintero, M., Guo, M., Geleynse, S., Ramasamy, K. K., et al. (2016). Unique low-molecular-weight lignin with high purity extracted from wood by deep eutectic solvents (DES): A source of lignin for valorization. *Green Chem.* 18, 5133–5141. doi:10.1039/c6gc01007e

Bjeli´c, A., Hoõcevar, B., Grilc, M., Novak, U., and Likozar, B. (2020). A review of sustainable lignocellulose biorefining applying (natural) deep eutectic solvents (DESs) for separations, catalysis and enzymatic biotransformation processes. *Rev. Chem. Eng.* 1, 243–272. doi:10.1515/revce-2019-0077

Björkman, A. (1954). Isolation of lignin from finely divided wood with neutral solvents. *Nature* 174, 1057–1058. doi:10.1038/1741057a0

Chen, Z., Bai, X., Lusi, A., and Wan, C. (2018). High-solid lignocellulose processing enabled by natural deep eutectic solvent for lignin extraction and industrially relevant production of renewable chemicals. *ACS Sustain. Chem. Eng.* 6 (9), 12205–12216. doi:10.1021/acssuschemeng.8b02541

Chen, Z., Ragauskas, A., and Wan, C. (2020). Lignin extraction and upgrading using deep eutectic solvents. *Ind. Crops Prod.* 147, 112241. doi:10.1016/j.indcrop.2020.112241

Cheng, J., Huang, C., Zhan, Y., Han, S., Wang, J., Meng, X., et al. (2022). Effective biomass fractionation and lignin stabilization using a diol DES system. *Chem. Eng. J.* 443, 136395. doi:10.1016/j.cej.2022.136395

Christopher, S. L., Sandra, C., Peter, dp., and Pieter, C. A. B. (2019). Linkage abundance and molecular weight characteristics of technical lignins by attenuated total reflection- FTIR spectroscopy combined with multivariate analysis. *ChemSusChem* 12, 1139–1146. doi:10.1002/cssc.201802809

Clarke, C. J., Tu, W. C., Levers, O., Brohl, A., and Hallett, J. P. (2018). Green and sustainable solvents in chemical processes. *Chem. Rev.* 118 (2), 747–800. doi:10.1021/acs.chemrev.7b00571

Dong, L., Lin, L., Han, X., Si, X., Liu, X., Guo, Y., et al. (2019). Breaking the limit of lignin monomer production via cleavage of interunit carbon–carbon linkages. *Chem* 13, 1521–1536. doi:10.1016/j.chempr.2019.03.007

Esmaeili, M., Anugwom, I., Manttari, M., and Kallioinen., M. (2018). Utilization of DES-lignin as a bio-based hydrophilicity promoter in the fabrication of antioxidant polyethersulfone. *Membranes* 8, 3. doi:10.3390/membranes8030080

Guo, D., Guo, Y., Sha, L., Lyu, G., Li, J., Zhang, X., et al. (2020). Subcritical ethanol catalyzed with deep eutectic solvent extract phenolic lignin for preparation of an ultraviolet-blocking composite film. *Energy fuels.* 34, 8395–8402. doi:10.1021/acs.energyfuels.0c00736

Hladnik, L., Vicente, F. A., Novak, U., Grilc, M., and Likozar, B. (2021). Solubility assessment of lignin monomeric compounds and organosolv lignin in deep eutectic solvents using *in situ* Fourier-transform infrared spectroscopy. *Ind. Crops Prod.* 164, 113359. doi:10.1016/j.indcrop.2021.113359

Laurichesse, S., and Averous, L. (2014). Chemical modification of lignins: Towards biobased polymers. *Prog. Polym. Sci.* 39, 1266–1290. doi:10.1016/j.progpolymsci.2013.11.004

Li, H. Y., Wang, B., Wen, J. L., Cao, X. F., Sun, S. N., and Sun, R. C. (2018). Availability of four energy crops assessing by the enzymatic hydrolysis and structural features of lignin before and after hydrothermal treatment. *Energy Convers. Manag.* 155, 58–67. doi:10.1016/j.enconman.2017.10.089

Liu, Y. R., Nie, Y., Lu, X. M., Zhang, X. P., He, H. Y., Pan, F. J., et al. (2019). Cascade utilization of lignocellulosic biomass to high-value products. *Green Chem.* 21, 3499–3535. doi:10.1039/C9GC00473D

Liu, Z., Wang, Z., Gao, S., Tong, Y., Le, X., Hu, N., et al. (2021). Isolation and fractionation of the tobacco stalk lignin for customized value-added utilization. *Front. Bioeng. Biotechnol.* 9, 811287. doi:10.3389/fbioe.2021.811287

Ma, C. Y., Gao, X., Peng, X. P., Gao, Y. F., Liu, J., Wen, J. L., et al. (2021a). Microwave-assisted deep eutectic solvents (DES) pretreatment of control and transgenic poplars for boosting the lignin valorization and cellulose bioconversion. *Ind. Crops Prod.* 164, 113415. doi:10.1016/j.indcrop.2021.113415

Ma, C. Y., Peng, X. P., Sun, S. L., Wen, J. L., and Yuan, T. Q. (2021b). Short-time deep eutectic solvents pretreatment enhanced production of fermentable sugars and tailored lignin nanoparticles from abaca. *Int. J. Biol. Macromol.* 192, 417–425. doi:10.1016/j.ijbiomac.2021.09.140

Ma, C. Y., Xu, L. H., Sun, Q., Sun, S. N., Cao, X. F., Wen, J. L., et al. (2022). Ultrafast alkaline deep eutectic solvent pretreatment for enhancing enzymatic saccharification and lignin fractionation from industrial xylose residue. *Bioresour. Technol.* 352, 127065. doi:10.1016/j.biortech.2022.127065

Monika, O., Mika, H. S., Bruno, D. M., and Orlando, J. R. (2020). Spherical lignin particles: A review on their sustainability and applications. *Green Chem.* 9, 2712–2733. https:// doi.org/doi:10.1039/d0gc00096e

Pu, Y., Hu, F., Huang, F., Davison, B. H., and Ragauskas, A. J. (2013). Assessing the molecular structure basis for biomass recalcitrance during dilute acid and hydrothermal pretreatments. *Biotechnol. Biofuels* 6, 15. doi:10.1186/1754-6834-6-15

Ralph, J., Lundquist, K., Brunow, G., Lu, F., Kim, H., Schatz, P. F., et al. (2004). Lignins: Natural polymers from oxidative coupling of 4-hydroxyphenyl-propanoids. *Phytochem. Rev.* 3, 29–60. doi:10.1023/b:phyt.0000047809.65444.a4

Rencoret, J., Marques, G., Gutierrez, A., Ibarra, D., Li, J., Gellerstedt, G., et al. (2008). Structural characterization of milled wood lignins from different eucalypt species. *Holzforschung* 62, 514–526. doi:10.1515/hf.2008.096

Sajjadi, M., Ahmadpoor, F., Nasrollahzadeh, M., and Ghafuri, H. (2021). Lignin-derived (nano) materials for environmental pollution remediation: Current challenges and future perspectives. *Int. J. Biol. Macromol.* 178, 394–423. doi:10.1016/j.ijbiomac.2021.02.165

Sanghamitra, S., Shradha, P., and Dimitris, S. A. (2015). Thermal properties of lignin in copolymers, blends, and composites: A review. *Green Chem.* 17, 4862–4887. doi:10.1039/c5gc01066g

Shen, X. J., Chen, T., Wang, H. M., Mei, Q., Yue, F., Sun, S., et al. (2019). Structural and morphological transformations of lignin macromolecules during bio-based deep eutectic solvent (DES) pretreatment. *ACS Sustain. Chem. Eng.* 8 (5), 2130–2137. doi:10.1021/acssuschemeng.9b05106

Siavash, I., and Rajender, S. V. (2020). Greener synthesis of lignin nanoparticles and their applications. *Green Chem.* 22, 612–636. doi:10.1039/c9gc02835h

Sluiter, A., Hames, B., Ruiz, R., Scarlata, C., Sluiter, J., Templeton, D., et al. (2008). *Determination of structural carbohydrates and lignin in biomass determination of structural carbohydrates and lignin in biomass laboratory analytical procedure (LAP)*. Battelle: National Renewable Energy Laboratory, U.S. Department of Energy Office of Energy Efficiency and Renewable Energy by Midwest Research Institute.

Sun, D., Wang, B., Wang, H. M., Li, M. F., Shi, Q., Zheng, L., et al. (2019). Structural elucidation of tobacco stalk lignin isolated by different integrated processes. *Industrial Crops Prod.* 140, 111631. doi:10.1016/j.indcrop.2019.111631

Torr, K. M., Love, K. T., Çetinkol, OP., Donaldson, L. A., George, A., Holmes, B. M., et al. (2012). The impact of ionic liquid pretreatment on the chemistry and enzymatic digestibility of Pinus radiata compression wood. *Green Chem.* 14, 778. doi:10.1039/c2gc16362d

Vin-Nnajiofor, M. C., Li, W. Q., Debolt, S., Cheng, Y. T., and Shi, J. (2022). Fractionation and upgrade of endocarp lignin to carbon- silicon nanocomposites as an anode material in lithium-ion batteries. *Appl. Eng. Agric.* 38 (3), 509–516. doi:10.13031/aea.14937

Wang, B., Sun, D., Wang, H. M., Yuan, T. Q., and Sun, R. C. (2018). Green and facile preparation of regular lignin nanoparticles with high yield and their natural broad-spectrum sunscreens. *ACS Sustain. Chem. Eng.* 7 (2), 2658–2666. doi:10.1021/acssuschemeng.8b05735

Wang, H. M., Wang, B., Wen, J. L., Wang, S. F., Shi, Q., and Sun, R. C. (2018). Green and efficient conversion strategy of Eucalyptus based on mechanochemical pretreatment. *Energy Convers. Manag.* 175, 112–120. doi:10.1016/j.enconman.2018.09.002

Wang, H. M., Sun, Y. C., Wang, B., Sun, D., Shi, Q., Zheng, L., et al. (2019a). Insights into the structural changes and potentials of lignin from bagasse during the integrated delignification process. *ACS Sustain. Chem. Eng.* 7 (16), 13886–13897. doi:10.1021/acssuschemeng.9b02071

Wang, H. M., Wang, B., Wen, J. L., Yuan, T. Q., and Sun, R. C. (2017). Structural characteristics of lignin macromolecules from different Eucalyptus species. *ACS Sustain. Chem. Eng.* 5 (12), 11618–11627. doi:10.1021/acssuschemeng.7b02970

Wang, H. M., Yuan, T. Q., Song, G. Y., and Sun, R. C. (2021). Advanced and versatile lignin-derived biodegradable composite film materials toward a sustainable world. *Green Chem.* 23 (11), 3790–3817. doi:10.1039/d1gc00790d

Wang, H. M., Wang, B., Sun, D., Shi, Q., Zheng, L., Wang, S., et al. (2019b). Unraveling the fate of lignin from Eucalyptus and poplar during integrated delignification and bleaching. *ChemSusChem* 12 (5), 1059–1068. doi:10.1002/cssc.201802592

Wang, H. M., Wang, B., Yuan, T., Lu, Z., Shi, Q., Wang, S., et al. (2020). Tunable, UV-shielding and biodegradable composites based on well-characterized lignins and poly(butylene adipate-co-terephthalate). *Green Chem.* 22, 8623–8632. doi:10.1039/d0gc03284k

Wang, L., Li, X., Jiang, J., Zhang, Y., Bi, S., and Wang, H. M. (2022). Revealing structural and functional specificity of lignin from tobacco stalk during deep eutectic solvents deconstruction aiming to targeted valorization. *Industrial Crops Prod.* 180, 114696. doi:10.1016/j.indcrop.2022.114696

Wen, J.-L., Sun, S.-L., Yuan, T.-Q., and Sun, R.-C. (2015). Structural elucidation of whole lignin from Eucalyptus based on preswelling and enzymatic hydrolysis. *Green Chem.* 17, 1589–1596. doi:10.1039/c4gc01889c

Wen, J.-L., Xue, B.-L., Xu, F., Sun, R.-C., and Pinkert, A. (2013a). Unmasking the structural features and property of lignin from bamboo. *Ind. Crops Prod.* 42, 332–343. doi:10.1016/j.indcrop.2012.05.041

Wen, J., Sun, S., Xue, B., and Sun, R. (2013b). Recent advances in characterization of lignin polymer by solution-state nuclear magnetic resonance (nmr) methodology. *Materials* 6, 359–391. doi:10.3390/ma6010359

Xu, J.-K., Zhou, P., Liu, X., Yuan, L., Zhang, C., and Dai, L. (2021). Tandem character of liquid hot water and deep eutectic solvent to enhance lignocellulose deconstruction. *ChemSusChem* 14, 2740–2748. doi:10.1002/cssc.202100765

Xi, Y. B., Yang, D. J., Wang, Y. Y., Huang, J. H., Yan, M. Z., Yi, C. H., et al. (2020b). Effect of structure of technical lignin on the electrochemical performance of lignin-derived porous carbon from K2CO3 activation. *Holzforschung* 74, 293–302. doi:10.1515/hf-2019-0107

Xu, J., Zhou, H., Zheng, Y., Li, C., Dai, L., Xu, C., et al. (2022). A rapid and reversible pH control process for the formation and dissociation of lignin nanoparticles. *ChemSusChem* 15 (8), e202200449. doi:10.1002/cssc.202200449

Zhang, R., Du, Q., Wang, L., Zheng, Z., Guo, L., Zhang, X. Y., et al. (2019). Unlocking the response of lignin structure for improved carbon fiber production and mechanical strength. *Green Chem.* 21, 4981–4987. doi:10.1039/c9gc01632e

Zhang, Z., Song, J., and Han, B. (2017). Catalytic transformation of lignocellulose into chemicals and fuel products in ionic liquids. *Chem. Rev.* 117, 6834–6880. doi:10.1021/acs.chemrev.6b00457

Zhao, W., Simmons, B., Singh, S., Ragauskas, A., and Cheng, G. (2016). From lignin association to nano-/micro-particle preparation: Extracting higher value of lignin. *Green Chem.* 18, 5693–5700. doi:10.1039/c6gc01813k

Zhao, X. B., Zhang, L., and Liu, D. (2012). Biomass recalcitrance. Part II: Fundamentals of different pretreatments to increase the enzymatic digestibility of lignocellulose. *Biofuel. Bioprod. Biorefin.* 6, 561–579. doi:10.1002/bbb.1350

Zhong, X., Yuan, R., Zhang, B., Wang, B., Chu, Y., and Wang, Z. (2021). Full fractionation of cellulose, hemicellulose, and lignin in pith-leaf containing corn stover by one-step treatment using aqueous formic acid. *Ind. Crops Prod.* 172, 113962. doi:10.1016/j.indcrop.2021.113962